Multidiszciplináris tudományok, 13. kötet. 4. sz. (2023), pp. 42–53 **https://doi.org/10.35925/j.multi.2023.4.5**

THERMAL PERFORMANCE ESTIMATION OF A V-CORRUGATED SOLAR AIR HEATER USING ANN TECHNIQUES

Mustafa Moayad Hasan
PhD student, University of Miskolc, Institute of Mathematics
3515 Miskolc, Miskolc-Egyetemváros, e-mail: hasan.mustafa.moayad@student.uni-miskolc.hu

Krisztián Hriczó
associate professor, University of Miskolc, Institute of Mathematics
3515 Miskolc, Miskolc-Egyetemváros, e-mail: krisztian.hriczo@uni-miskolc.hu

Abstract

A solar air heater (SAH) is a unique form of solar thermal collector that utilizes solar energy emitted from the sun to produce heated air. Various experimental and theoretical investigations have been undertaken to improve the poor thermal performance of SAHs. The difficulties related to these studies drew attention toward a reliable soft computing technique exemplified by the Artificial Neural Network (ANN) technique. The current work applied actual meteorological data from Miskolc City, Hungary, to an ANN model with the structure of a Multi-layer Perceptron (MLP) to forecast the energy performance of a V-corrugated solar-powered air heater. Seven input parameters and one output parameter make up the ANN structure, with a single hidden layer. For the purpose of selecting the most effective network for predicting output parameters, ten neurons have been assessed. The suggested ANN model was trained with 336 data sets using the Levenberg-Marquardt (LM) learning technique. The comparison of anticipated and real thermal performance values shows a very good agreement. The statistical error analysis showed that the optimal ANN model structure of 7-8-1 can reliably and accurately predict SAH's thermal performance and thus it can save both time and cost.

Keywords: *solar air heater, thermal performance, artificial neural network, Levenberg–Marquardt algorithm, multi-layer perceptron*

1. Introduction

The reliance on fossil fuels has resulted in several issues, including the effects of greenhouse gases, the loss of the ozone layer, the consequences of acid rain, and air pollution. The limited quantities of this source of energy will cause a drastic depletion in the near future (Hamdan et al., 2016). Consequently, renewable and alternative sources of energy have been profoundly investigated. The most distinctive form of renewable energy is solar energy. It is an environmentally friendly, accessible, sustainable, and carbon-free energy source (Bazri et al., 2019). Solar systems can be categorized into three main types: which are solar thermal systems(ST), solar photovoltaic systems (PV), and dual (hybrid) systems Figure 1.

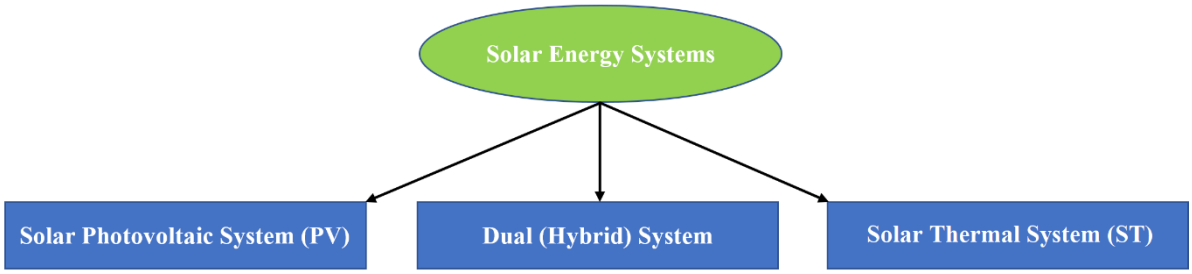

Figure 1. *Classification of solar energy systems.*

A solar thermal device is one such structure that is designed to harvest and convert the emitted heat energy from the sun into usable thermal energy using an essential component called a solar collector. In general, solar collectors are classified into liquid and air collectors depending on the type of heat transfer medium (Vengadesan and Senthil, 2020).

The solar air collector (SAC) plays a crucial role in various applications such as space heating, agricultural drying, and other applications in industry (Hasan and Hriczó, 2023). The primary limitations of a SAC arise from the inadequate thermal conductivity and insufficient heat capacity of air. Consequently, this leads to a reduced heat transfer coefficient between the flowing air and absorber plate, resulting in a lower thermal efficiency of the collector. Recently, various numerical and experimental studies have been carried out by numerous researchers to ameliorate the thermal performance of SACs (Karim and Hawlader, 2004; Karsli, 2007; Benli, 2013). Experimental investigation of the thermal performance of solar collectors consumes both time and effort due to various measurements. Additionally, the numerical methods commonly employed for estimating the thermal performance of SACs often require substantial computational power and significant time to generate accurate predictions. Soft computing techniques can address these concerns while saving time and money. The Artificial Neural Network (ANN) has gained significant popularity across various disciplines, particularly in engineering applications. This is primarily due to its faster computation performance and excellent outcomes, making it a superior technique in comparison (Ghritlahre, 2018). Researchers have increasingly employed ANN in thermal engineering applications recently (Ghritlahre et al., 2021).

In the current study, the ANN approach has been employed to predict the solar energy efficiency of a V-corrugated SAC. The ANN structure is a multi-layer perceptron (MLP) form with a single hidden layer, seven input parameters and one output parameter. The ANN model was assessed using real weather data from Miskolc City, Hungary. A total of 336 data sets are implemented in this ANN model. These data are divided into training, validation, and testing groups. The suggested ANN model underwent training using the Levenberg–Marquardt (LM) learning approach to forecast the thermal performance of SAC. In order to detect the suitable network for predicting output parameters, the study examined the range of 3-12 neurons in the hidden layer. Through error analysis, it has been found that a network with eight neurons in the hidden layer, utilizing the LM algorithm, yielded the best results. In addition, the study involved a comparison between the predicted and actual values of thermal performance. Furthermore, a statistical error analysis was conducted specifically for the predicted values of thermal performance.

2. Energy analysis of solar air heater

The thermal efficiency (η) of any solar thermal device is a key indicator of its performance. It is defined as the ratio of the useful heat gain (Q_u) to the total incident solar irradiation (I_t) and it is calculated as (Duffie et al., 2020):

$$\eta = \frac{Q_u}{A_c\, I_t} \tag{1}$$

where A_c is the collector area and I_t is the total incident radiation.
The useful heat gain of a collector (Q_u) can be calculated by subtracting the overall thermal losses (U_l) from the absorbed solar radiation (S) as (Duffie et al., 2020):

$$Q_u = A_c F_R [S - U_l(T_i - T_a)] \tag{2}$$

where F_R is the collector heat removal factor, T_i is the air inlet temperature, and T_a is the ambient temperature. The absorbed solar energy by the collector (S) can be calculated on an hourly basis using the following equation (Duffie et al., 2020):

$$S = D_f\, .S_f\, [I_b(\tau\alpha)_{eb} + I_d(\tau\alpha)_{ed} + I_r(\tau\alpha)_{er}] \tag{3}$$

where, I_b, I_d, and I_r are the beam, diffuse, and the ground reflected radiation, respectively which are briefly calculated by Ref. (Duffie et al., 2020). $(\tau\alpha)_{eb}$, $(\tau\alpha)_{ed}$, and $(\tau\alpha)_{er}$ are the effective transmittance-absorbtance product for beam, diffuse, and ground reflected solar radiation, respectively. The dust factor D_f which accounts for the reduction in absorber energy due to dust on the glass cover was assumed equal to (0.99), while the shade factor S_f which accounts for the reduction in absorbed energy when some of the air heater structure intercepts solar radiation was assumed (0.98). The term $U_l(T_i - T_a)$ is the thermal losses with details of calculation given in Ref. (Duffie et al., 2020). The collector heat removal factor (F_R) quantifies the ratio of the actual useful energy collected to the energy that would be collected if the entire absorber plate were at the temperature of the fluid entering the collector. It can be calculated as (Duffie et al., 2020):

$$F_R = \frac{G\, c_p}{U_l}\left[1 - exp\left(\frac{-F' U_l}{G\, c_p}\right)\right] \tag{4}$$

where, G is the air mass flux, and F' is the collector efficiency factor.

3. Artificial Neural Network (ANN)

In the field of artificial intelligence (AI), the most widely utilized technique is the artificial neural network (ANN) (Qazi et al., 2015). The structure of ANN is similar to that of the human nervous system and it works like a human brain. It aims to emulate the functions of the human brain in a computerized manner by learning the connections between input and output through training, where the network adjusts its parameters to optimize performance and improve its ability to make accurate predictions or classifications. Therefore, it operates like a black box model. The ANN's general structure is composed of three major layers: an input layer, one or more hidden layers, and an output layer as shown in Figure 2.

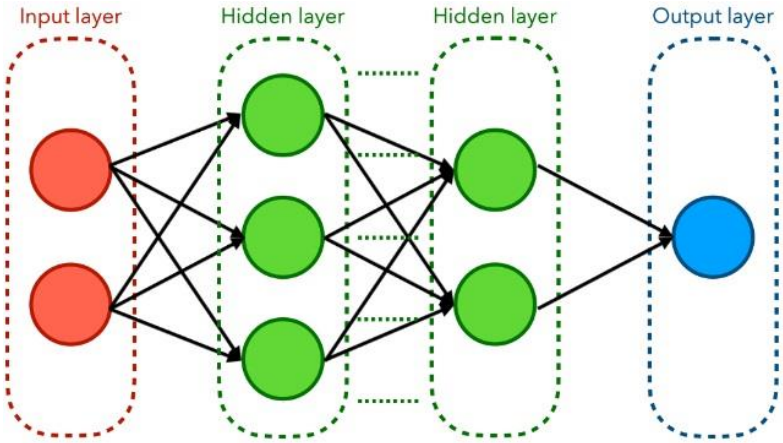

Figure 2. *The structure of an artificial neural network.*

This structure is known as the multi-layered perceptron (MLP) model and it is the most popular one (˙I¸seri and Karlık, 2009). Each layer contains of several tiny, individually linked processing components known as neurons or nodes. The number of nodes in the input and output layers is dictated by the quantity of parameters present in those layers. Basically, ANN operates in two stages: the initial stage involves the learning process, while the subsequent stage involves storing data sets within interconnections referred to as weights. The ANN tool is commonly utilized to predict outcomes by considering factors such as income, the neural model structure, and the chosen learning approaches. Levenberg-Marquardt (LM), Polak-Ribiere Conjugate Gradient (CGP), One Step Secant (OSS), Scaled Conjugate Gradient (SCG), and BFGS Quasi-Newton (BFG) are only a few examples of learning algorithms that can be used for model training (Ghritlahre et al., 2021). LM is the standout algorithm among these options, as it is derived from the original Newton algorithm and is designed to solve minimization problems. It offers improved stability, efficiency, and rapid convergence while keeping the discrepancies between actual and expected values to a minimum. (Benli, 2013).

ANN is a MATLAB simulation tool that stands out for its speed, simplicity, and ability to handle multiple values. It excels at solving intricate relationships between these values and providing accurate predictions, even when trained with limited data (Esen et al., 2009).

4. Levenberg–Marquardt training algorithm

The LM algorithm is a refined version of Newton's method that effectively minimizes functions consisting of sums of nonlinear functions' squares (Demuth and Beale, 2003). Its development aimed to overcome the limitations of both the Gauss-Newton (GN) method and the gradient descent algorithm, making it a valuable intermediate optimization technique.

The GN method exhibits an impressive quick quadratic convergence, but it heavily relies on the accurate selection of weight values, which may not be practically feasible for real-world problems. In contrast, the gradient descent algorithm is less reliant on initial values but converges at a slower pace. However, its linear approach towards the minimum can sometimes lead to a sluggish convergence rate and insufficient convergence properties.

The LM algorithm is a hybrid optimization technique that combines the positive attributes of GN and gradient descent algorithms. It is suitable for many real-world applications. This algorithm possesses

quadratic convergence, which means it approximates the GN method when it is in the vicinity of a minimum (but not too close) (Kollias and Anastassiou, 1989). To improve the accuracy of its parameters, LM uses gradient descent to enhance an initial guess. As it approaches the minimum value of the cost function, it transforms to the GN method. Once it reaches the minimum, it transforms back to the gradient descent algorithm to further improve accuracy. The update rule for the weights of the neural network according to GN method is (Kermani et al., 2005):

$$\Delta\omega \;=\; -[\nabla^2 E(\omega)]^{-1}.\nabla E(\omega) \tag{5}$$

where $\nabla^2 E(\omega)$ represents the Laplacian of the energy function and is also referred to as the Hessian matrix. The Hessian term can be written as:

$$\nabla^2 E(\omega) \;=\; J^{\mathrm{T}}(\omega).J(\omega) \;+\; S(\omega) \tag{6}$$

$$S(\omega) \;=\; \sum_{\mathrm{i}=1}^{\mathrm{N}} e_{\mathrm{i}}(\omega)\,.\,\nabla^2 e_{\mathrm{i}}(\omega) \tag{7}$$

where the term $e_{\mathrm{i}}(\omega)$ denotes the error vector of the neural network for pattern i and $J(\omega)$ represents the Jacobian matrix.

Similar to the Taylor partial series expansion, for the GN method it is normally assumed that:

$$S(\omega) \;\approx\; 0 \tag{8}$$

The term $S(\omega)$ includes the second derivatives of the network error concerning the network weights. Calculating this term is costly since the number of computations grows exponentially as the size of the network increases. By merging the equations above, we can formulate the update rule for the GN method as:

$$\Delta(\omega) \;=\; -[J^T(\omega).J(\omega)\,]^{-1}.J^T(\omega).e(\omega) \tag{9}$$

Given the above introduction, the Levenberg–Marquardt modification to the GN method is as follows:

$$\Delta(\omega) = -[J^T(\omega).J(\omega) + \lambda I]^{-1}.J^T(\omega).e(\omega) \tag{10}$$

It's worth noting that the expression above is an approximation of gradient descent, using a learning rate of $1/\lambda$ when λ is large. Conversely, the algorithm approximates the GN method when λ is small. The LM algorithm is unique in its ability to adjust the λ parameter adaptively, enabling it to navigate between these two extremes effectively. This approach combines the strengths of both gradient descent and GN algorithms while avoiding their limitations. The adaptive adjustment of the λ parameter is similar to the adaptive learning rate modification in the back-propagation algorithm. When a step leads to an increased energy function, λ is multiplied by a constant $\lambda_{Inc} > 1$, moving the algorithm in the direction of the gradient descent algorithm for more stability. On the other hand, if a step leads to a decreased energy function, λ is multiplied by $\lambda_{\mathrm{Dec}} = 1/\lambda_{Inc}$, moving the algorithm towards the GN algorithm and gaining more speed (Singh et al., 2007).

5. Modeling of ANN structure

In the present work, the data is partitioned into three subsets during the modeling process: The training set is utilized to calculate and adjust the weights and biases of the network. The validation set is employed to monitor errors during the training phase. The MLP structure was devised specifically in order to anticipate the energy performance of SAH. For ANN structure development, seven parameters: date, time, solar radiation intensity, ambient temperature, mean plate temperature, outlet collector temperature, and air mass flow rate are used in the input layer. The output layer is dedicated to representing the energy efficiency of SAH. The three-layer network structure is shown in Figure 3.

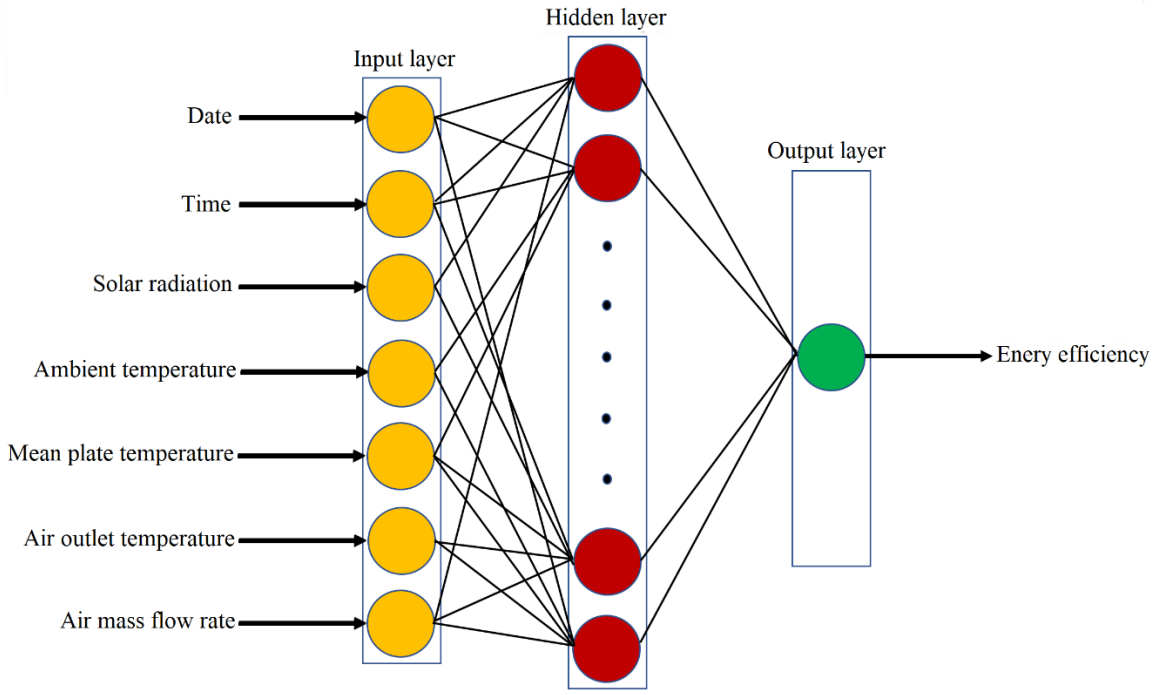

Figure 3. *The structure of ANN in the present study.*

A total of 336 samples were collected for the MLP model used for prediction. In total, 70% of these samples were employed for training, 15% for validation, and the remaining 15% for testing purposes. Prior to inputting the data into the model, a normalization process was applied to ensure values fell within the range of 0 and 1. The selection of the number of neurons in the hidden layer was primarily determined through a trial and error approach. Accordingly, 3 to 12 neurons have been examined to assess any performance enhancements achieved by the proposed modeling system.

6. Results and discussion

For modeling purposes, a feed-forward neural network based on the back propagation algorithm was employed. This algorithm serves as a training function for the network, where it updates the weight and bias values using the LM back propagation optimization method (˙I¸seri and Karlık, 2009). The performance evaluation of each model with a range of 3 to 12 hidden neurons was conducted using statistical error analysis. Table 1 presents the results of the statistical analysis for the model.

Table 1. *Statistical evaluation of MLP with 3-12 hidden neurons.*

LM	MSE1	MSE2	MSE3	R1	R2	R3	Rt
3	3.93E-04	4.35E-04	4.41E-04	0.99854	0.99813	0.99836	0.99844
4	1.40E-04	1.55E-04	2.78E-04	0.99948	0.99943	0.99872	0.99938
5	4.38E-06	5.38E-06	4.94E-06	0.99998	0.99997	0.99998	0.99998
6	9.63E-05	1.24E-04	1.32E-04	0.99963	0.99956	0.99944	0.9996
7	3.15E-05	5.91E-05	5.88E-05	0.99988	0.99982	0.9998	0.99985
8	**2.99E-06**	**3.20E-06**	**4.53E-06**	**0.99999**	**0.99999**	**0.99998**	**0.99999**
9	4.11E-06	4.90E-06	1.39E-05	0.99998	0.99998	0.99995	0.99998
10	4.81E-06	1.06E-05	8.79E-06	0.99998	0.99996	0.99997	0.99998
11	1.04E-05	1.97E-05	1.29E-05	0.99996	0.99993	0.99995	0.99995
12	1.78E-05	6.45E-05	3.94E-05	0.99993	0.99976	0.99986	0.99989

It can be observed that the MLP model with 8 hidden neurons exhibited the lowest mean square error (MSE) and the highest correlation coefficient (R). Training, validation, testing, and overall period correlation coefficients were exceptionally high, with values of 0.99999, 0.99999, 0.99998, and 0.99999, respectively. These values surpassed those of other models with varying neuron counts, indicating superior performance. Additionally, the model achieved the lowest MSE values for training, validation, and testing, measuring 2.99E-06, 3.20E-06, and 4.53E-06, respectively.

In Figure 4, the performance curve of a 7-8-1 neuron model is illustrated. The graph demonstrates a consistent decrease in MSE values as the number of epochs increases. The training process concluded at epoch 252 since it had the lowest MSE among the validation sets. Notably, the most accurate value of the predicted results from the Artificial Neural Network (ANN) was obtained at epoch 258, which exhibited a remarkably minimal MSE and indicated the best validation performance.

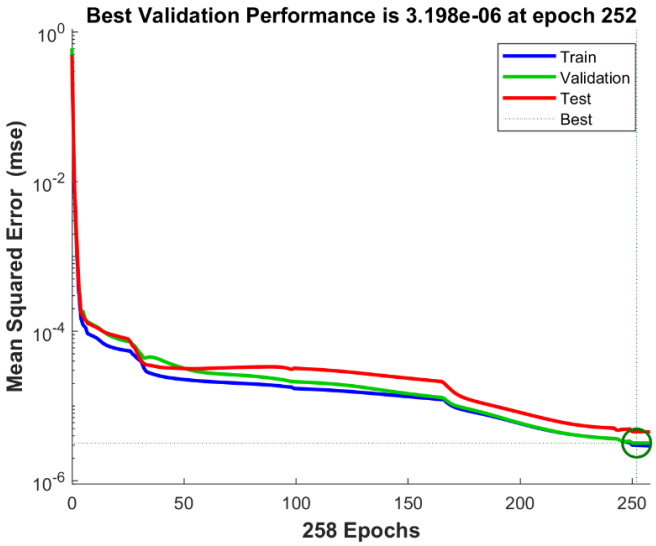

Figure 4. *Performance curve of 7-8-1.*

The histogram of the errors is shown in Figure 5. It reflects the prediction accuracy of the ANN model. The histogram confirms that a significant portion of the errors are concentrated around the zero-

point error line. This observation further strengthens the notion that the ANN model accurately predicted the performance of SAH.

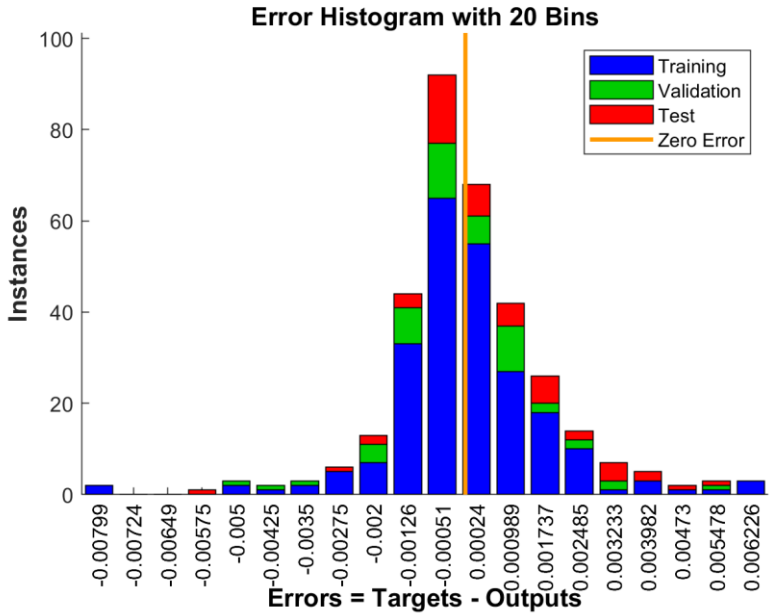

Figure 5. *Histogram of errors in proposed MLP of 7-8-1.*

Figure 6 displays the regression plot of the model with a 7-8-1 structure. The regression coefficient (R) values for training, validation, testing, and the overall process are found to be optimal. The circles in this diagram indicate data points, while the colored lines reflect the best match between outputs and targets. Notably, the outputs are perfectly aligned with the targets, indicating that the ANN's MLP structure can forecast the performance of SAH with a high level of accuracy.

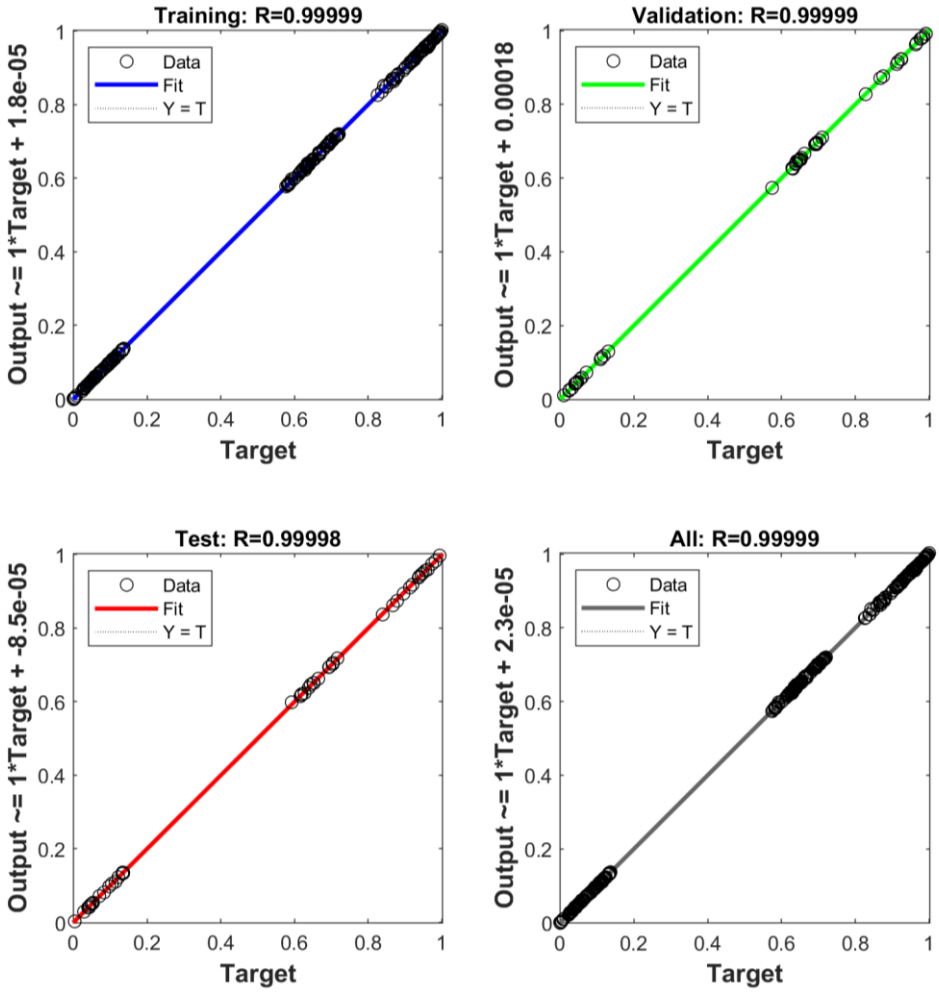

Figure 6. *The Regression plot of an artificial neural network.*

The comparison between actual (target) and predicted (output) thermal efficiency is illustrated in Figure 7. Additionally, the discrepancy between these two values is displayed in the form of a bar chart in Figure 8. The maximum error value is 0.0066 and the minimum error value is -0.0084, which are recorded at sample numbers of 217 and 316, respectively.

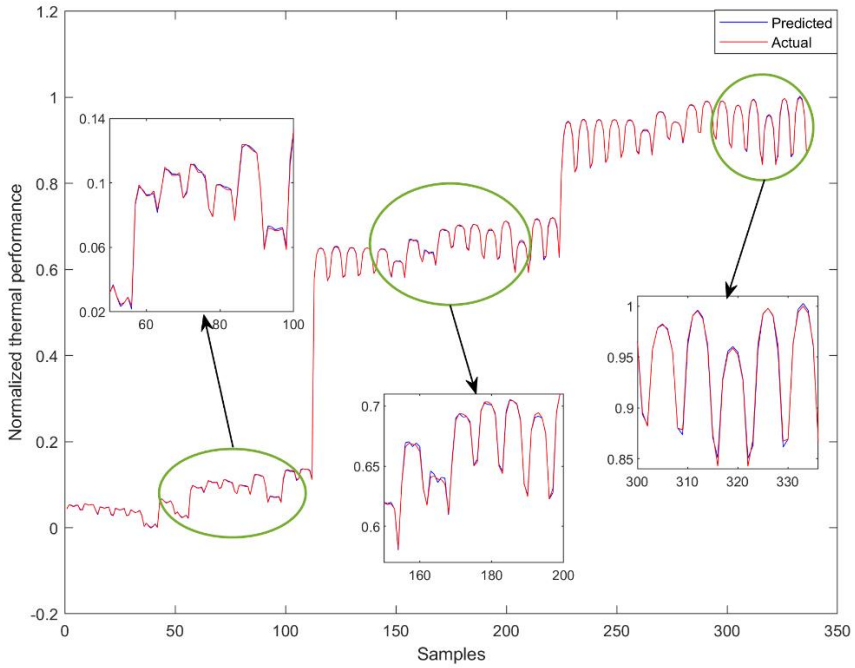

Figure 7. *Comparison between actual and anticipated thermal performances.*

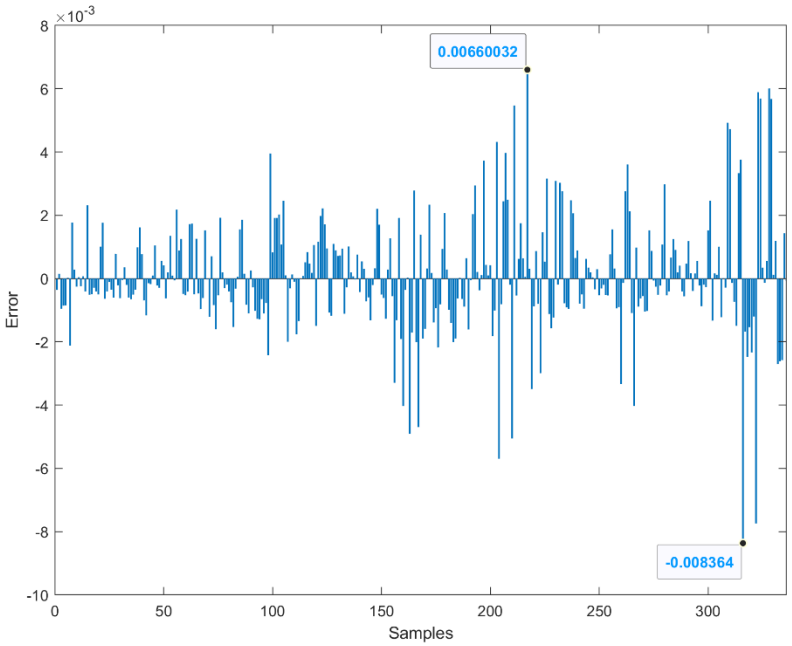

Figure 8. *Individual error bar graph.*

7. Summary

In this paper, an ANN model was built using the LM learning technique and effectively used to forecast the energy efficiency of a V-corrugated SAH. In total, 336 data sets were employed to examine the neural model. The neural model utilized seven parameters in the input layer and one parameter in the output layer. In the hidden layer, various numbers of neurons ranging from 3 to 12 were tested. By performing statistical error analysis, it was identified that the optimal number of neurons in the hidden layer for the neural model is 8, as evidenced by the lowest mean square error (MSE) and the highest correlation coefficient (R) among all evaluated neurons. Moreover, the statistical error analysis confirms the ANN model's dependability and correctness.

According to the results obtained, our 7-8-1 ANN model possesses the capability to precisely estimate the intricate relationship between input and output parameters. The robustness of this ANN model in predicting the energy efficiency of SAH is evident from the histogram and regression plots, further validating its effectiveness.

In view of the high level of precision achieved in anticipating the energy efficiency of SAH, the proposed MLP neural network model can be applied to properly forecast the thermal performance of the SAH systems. Therefore, it can be concluded that our 7-8-1 ANN model can be used as an alternative way since this technique requires less time and a number of tests as compared to other experimental and analytical approaches that are expensive and entail sophisticated governing formulas. This approach provides an easy and cost-effective method for manufacturers to simulate SAH, saving both time and expenses.

References

[1] Hamdan, M., Abdelhafez, E., Hamdan, A., and Haj Khalil, R. (2016). Heat transfer analysis of a flat-plate solar air collector by using an artificial neural network. *Journal of infrastructure systems*, 22(4), A4014004. **https://doi.org/10.1061/(ASCE)IS.1943-555X.0000213**

[2] Bazri, S., Badruddin, I. A., Naghavi, M. S., Seng, O. K., and Wongwises, S. (2019). An analytical and comparative study of the charging and discharging processes in a latent heat thermal storage tank for solar water heater system. *Solar Energy*, 185, 424–438. **https://doi.org/10.1016/j.solener.2019.04.046**

[3] Vengadesan, E., and Senthil, R. (2020). A review on recent developments in thermal performance enhancement methods of flat plate solar air collector. *Renewable and Sustainable Energy Reviews*, 134, 110315. **https://doi.org/10.1016/j.rser.2020.110315**

[4] Hasan, M. M., and Hriczó, K. (2023). A literature review of a dual-purpose solar collector. *Vehicle and Automotive Engineering*, 302–321. **https://doi.org/10.1007/978-3-031-15211-5_26**

[5] Karim, M., and Hawlader, M. (2004). Development of solar air collectors for drying applications. *Energy conversion and management*, 45(3), 329–344. **https://doi.org/10.1016/S0196-8904(03)00158-4**

[6] Karsli, S. (2007). Performance analysis of new-design solar air collectors for drying applications. *Renewable Energy*, 32(10), 1645–1660. **https://doi.org/10.1016/j.renene.2006.08.005**

[7] Benli, H. (2013). Determination of thermal performance calculation of two different types solar air collectors with the use of artificial neural networks. *International Journal of Heat and Mass Transfer*, 60, 1–7. **https://doi.org/10.1016/j.ijheatmasstransfer.2012.12.042**

[8] Ghritlahre, H. K. (2018). Development of feed-forward back-propagation neural model to predict the energy and exergy analysis of solar air heater. *Trends in Renewable Energy*, 4(2), 213–235. **https://doi.org/10.17737/tre.2018.4.2.0078**

[9] Ghritlahre, H. K., Chandrakar, P., and Ahmad, A. (2021). A comprehensive review on performance prediction of solar air heaters using artificial neural network. *Annals of Data Science*, 8(3), 405–449. **https://doi.org/10.1007/s40745-019-00236-1**

[10] Duffie, J. A., Beckman, W. A., and Blair, N. (2020). *Solar engineering of thermal processes, photovoltaics and wind*. John Wiley & Sons.

[11] Qazi, A., Fayaz, H., Wadi, A., Raj, R. G., Rahim, N. A., and Khan, W. A. (2015). The artificial neural network for solar radiation prediction and designing solar systems: A systematic literature review. *Journal of Cleaner Production*, 104, 1–12. **https://doi.org/10.1016/j.jclepro.2015.04.041**

[12] ˙I¸seri, A., and Karlık, B. (2009). An artificial neural networks approach on automobile pricing. *Expert Systems with Applications*, 36(2), 2155–2160. **https://doi.org/10.1016/j.eswa.2007.12.059**

[13] Esen, H., Ozgen, F., Esen, M., and Sengur, A. (2009). Artificial neural network and wavelet neural network approaches for modelling of a solar air heater. *Expert systems with applications*, 36(8), 11240–11248. **https://doi.org/10.1016/j.eswa.2009.02.073**

[14] Demuth, H., and Beale, M.: *Neural network design*, 2003 7th International Student Edition.

[15] Kollias, S., and Anastassiou, D. (1989). An adaptive least squares algorithm for the efficient training of artificial neural networks. *IEEE Transactions on Circuits and Systems*, 36(8), 1092–1101. **https://doi.org/10.1109/31.192419**

[16] Kermani, B. G., Schiffman, S. S., and Nagle, H. T. (2005). Performance of the Levenberg–Marquardt neural network training method in electronic nose applications. *Sensors and Actuators B: Chemical*, 110(1), 13–22. **https://doi.org/10.1016/j.snb.2005.01.008**

[17] Singh, V., Gupta, I., and Gupta, H. (2007). Ann-based estimator for distillation using Levenberg–Marquardt approach. *Engineering Applications of Artificial Intelligence*, 20(2), 249–259. **https://doi.org/10.1016/j.engappai.2006.06.017**